Mapping interplanetary weather

A. Hewish

During the last thirty years observations made on spacecraft travelling far beyond the magnetosphere have greatly advanced our knowledge of conditions in space between the Sun and the Earth. However, spacecraft can only sample the solar wind locally and there are generally so few of them present at any one time that it is not possible to obtain a global view of interplanetary weather patterns. Ground-based observations of a large grid of radio galaxies are now being used to map disturbances as they move across interplanetary space and this novel technique is providing new insights into the phenomena of interplanetary weather.

SPACE weather conditions in the near-Earth environment are of considerable importance to spacecraft operations. Several geostationary satellites are known to have failed because of solar-terrestrial disturbances during which bombardment by energetic charged particles has damaged electronic circuits. A recent example was the failure of the geostationary satellites Anik E-1 and E-2 in January, 1994. In March 1989 the US space shuttle Discovery was launched into a major geomagnetic storm and its mission life was seriously reduced by the malfunction of an on-board computer.

Dramatic increases in the temperature, which can double in a few hours, cause large variations in the upper-atmospheric density increasing the drag on satellites, resulting in difficult tracking and reducing the accuracy of satellite-based navigational systems. On the Earth's surface, rapid geomagnetic fluctuations during magnetic storms induce currents in power lines which are important at high latitudes. Both Toronto and Quebec have been blacked-out by the breakdown of their power distribution systems due to this cause. Since the earliest days of radio communication it has been known that disturbances in the ionosphere, during which breakdowns of radio links frequently occur, are yet another manifestation of geomagnetic storms. These are some of the reasons why we need to know more about space weather and how it depends upon events at the Sun.

Local space weather is intimately related to the behaviour of the solar wind, but in spite of intensive research aimed at better predictions, the solar origins of geo-effective disturbances are still poorly understood and accurate predictions are not yet possible. A major difficulty is the lack of observational data on the propagation of disturbances between the Sun and the Earth. Spacecraft have penetrated to roughly one third of the Sun–Earth distance and recorded in great detail the physical nature of the interplanetary shocks and solar wind streams that they encountered but it would require a large fleet of spacecraft to obtain a global view of interplanetary weather patterns. A relatively new technique which is now beginning to fill this gap is a spin-off from radioastronomy based on interplanetary scintillation.

We discovered at Cambridge in 1964 that certain radio galaxies and quasars exhibit rapid variations of intensity caused by small-scale variations of plasma density in the solar wind[1]. Only those sources having angular sizes of less than about one arcsec showed the effect, which is readily understood in terms of simple diffraction theory. Scintillation can only occur when the scale of the turbulence is less than a few hundred km, and in this case sources having a larger angular size smear out the scintillation pattern. On suitable radio sources scintillation can be seen in any direction in the sky although it is stronger when the line of sight passes nearer to the Sun. Following the discovery it was immediately realized that interplanetary scintillation provided a new method for estimating the angular sizes of radio sources and also for observing the solar wind.

Ground-based measurements of the solar wind speed were made by observing the motion of the scintillation pattern using three spaced antennas. An advantage of this method is that, unlike spacecraft measurements, observations can be made far from the ecliptic plane and it was soon found that the Sun emitted a faster wind from the polar regions[2]. Only now in 1994 is the spacecraft Ulysses beginning to make the first out-of-ecliptic measurements confirming the discovery. Systematic observations throughout the solar cycle using the scintillation method have already shown that the stream of high-speed wind from the poles becomes progressively narrower towards sunspot maximum and almost disappears when the Sun reverses its dipole magnetic field[3].

Measurements of the speed of the solar wind can be made with relatively small antennas since only a modest

A. Hewish is in the Cavendish Laboratory, Madingley Road, Cambridge CB3 0HE, UK.

Based on the lecture given at the Indian Institute of Science, Bangalore.

number of the most intensive radio sources needs to be observed. Day to day mapping of weather patterns, on the other hand, requires data on about 1000 sources in order to provide sufficient sky-coverage and this demands a dedicated antenna of high sensitivity.

The mapping technique

Intensity scintillation caused by small-scale turbulence in the solar plasma has a typical timescale of about one second and is best observed at metre wavelengths. Estimation of the degree of scintillation to 10% accuracy therefore involves observing a source for at least 100s, so the requirement for recording 1000 sources each day demands some multiple beam system. The Cambridge array operates at 81.5 MHz and contains 4096 full-wave dipoles covering an area of 36,000 m^2. The dipoles are arranged in 32 rows of 128 dipoles, and the northern and southern halves of the array, each containing 16 rows, are combined as an interferometer[4]. Sources are observed for a few minutes at meridian transit and phase-scanning using Butler matrices provides 16 beams covering the full range of declination simultaneously. Intensity fluctuations in the band 0.1 –3.0 Hz are filtered, integrated and sampled at 10s intervals. These 16 data-streams form the basis for constructing daily maps of interplanetary weather.

Having chosen a suitable grid of about 1000 sources from a catalogue[5] derived from previous sky surveys, the next stage is to make a calibration curve for each source. When day to day variations are averaged out, the scintillation for a typical source depends upon the solar elongation of the line of sight as shown in Figure 1. The systematic increase with decreasing elongation follows to the radial variation of mean plasma density $N \alpha r^{-2}$, where r is distance from the Sun. Near elongation 30° the curve flattens and then falls away. This is due to the saturation of scintillation, and an associated decrease in transverse scale of the diffraction pattern at the Earth which results in a progressive blurring of the pattern due to the angular diameter of the source. Since sources have different angular sizes causing different amounts of blurring, individual calibration curves are needed for each source.

A convenient measure of the day to day variations of scintillation is the ratio of the observed scintillation to the expected value derived from the calibration curve in which the short term variations have been smoothed out. This ratio, called the g-factor, removes the systematic dependence of scintillation upon the radial gradient of mean density. When enough g-values over the sky on any day have been obtained it is possible to map large-scale disturbances as illustrated schematically in Figure 2.

The region of space in the Earth's vicinity within which disturbances of density should be detectable by scintillation mapping can be determined by adopting a suitable model for the average distribution of turbulence around the Sun. Such a model specifies the physical scale and magnitude of the small-scale turbulent density variations in terms of radial distance from the Sun, and can be derived from a wide variety of scintillation observations made at different radio frequencies and solar elongations[6].

If ds^2 is the mean square intensity scintillation due to an element dz along the line of sight, where z is distance from the Earth, then for an undisturbed solar wind of average density we have $ds^2 = \beta(r)\, F(z)\, dz$ where $\beta(r)$ is the model defining the turbulence and $F(z)$ is a diffraction function which takes care of source-blurring and the dependence of scintillation upon distance from the element. The total intensity scintillation ΔS^2 is then obtained by integration along the line of sight so that

$$\Delta S^2 = \int_0^\infty \beta(r) F(z)\, dz. \qquad (1)$$

In the presence of a disturbance, which can be expressed as a modulation of the mean density over some region of space defined by a numerical factor $G(r, \theta, \phi)$, we then have

$$\Delta S^2 = \int_0^\infty G(r, \theta, \phi)\, \beta(r)\, F(z)\, dz, \qquad (2)$$

where it has been assumed that $G(r, \theta, \phi)$ is not large enough to cause saturation of scintillation.

The overall zone within which typical disturbances should be detectable is easily derived from the form of the weighting function given in (1). For an average source diameter of 0·5 arcsec the weighting function is shown in Figure 3 where the grey-scale has been normalized to remove the systematic increase of scintillation with decreasing solar elongation of the line of sight. This is the weighting function required when computing g-maps for given disturbances $G(r, \theta, \phi)$. As seen from Figure 3, the scintillation is largely due to regions extending to distances of about 1 AU from the Earth, the dominant zone lying between about 0·1 AU to 0·6 AU. Evidently scintillation is not sensitive to disturbances travelling outwards from the solar limb and is most sensitive to those within about ±45° of the Sun–Earth line.

Mapping corotating streams

The mapping technique is well exemplified at times when the solar wind is relatively stable and characterized by a small number of long-lived streams. Such conditions are typically found when the solar disk is free from active regions associated with sunspot groups. Streams of high speed and low plasma density are emitted from coronal holes which are seen as zones of low intensity in soft X-ray images of the solar corona. Except for

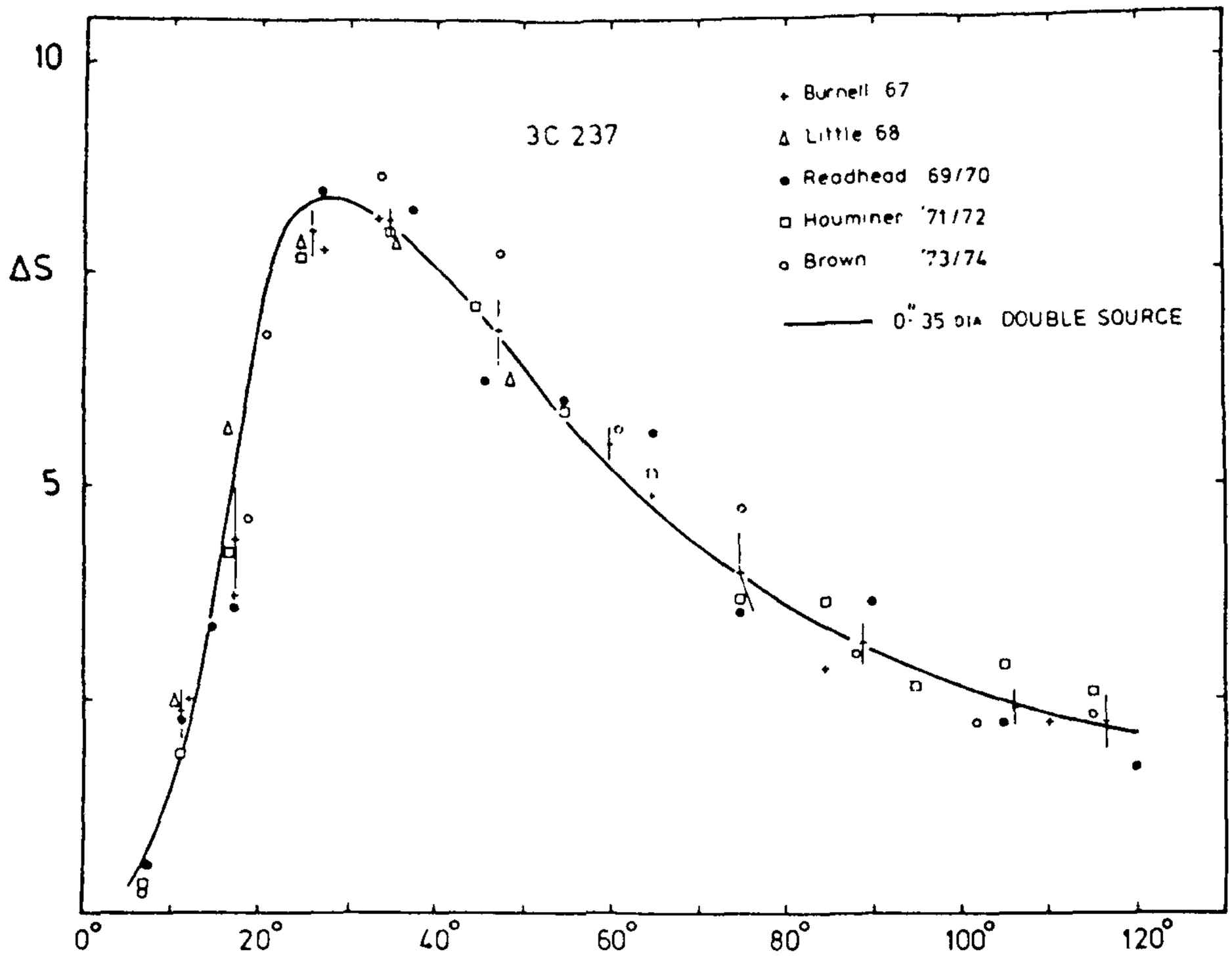

Figure 1. The root mean square scintillating flux density, ΔS, for a typical radio source plotted against solar elongation. The observations cover 1967–74 and day to day variations have been averaged

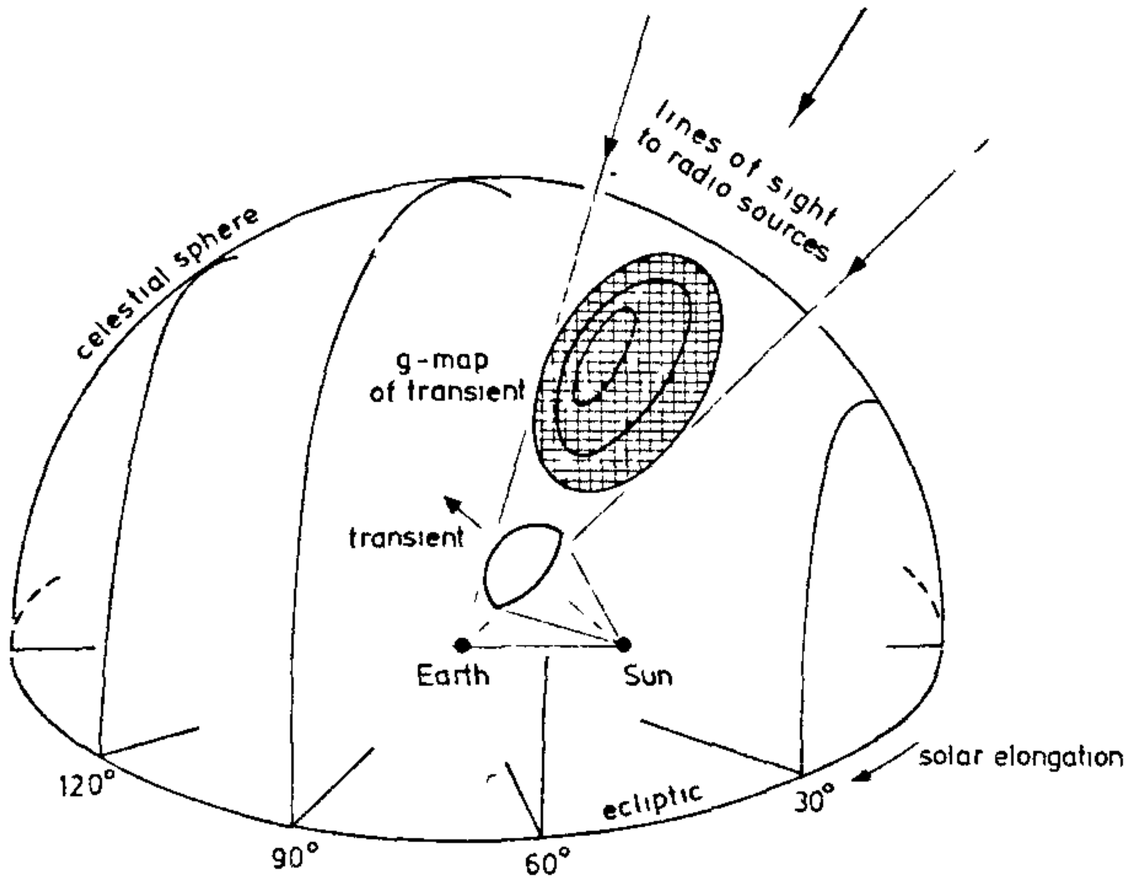

Figure 2. Schematic diagram of the scintillation mapping technique showing the two-dimensional projection of a solar transient projected against the celestial sphere.

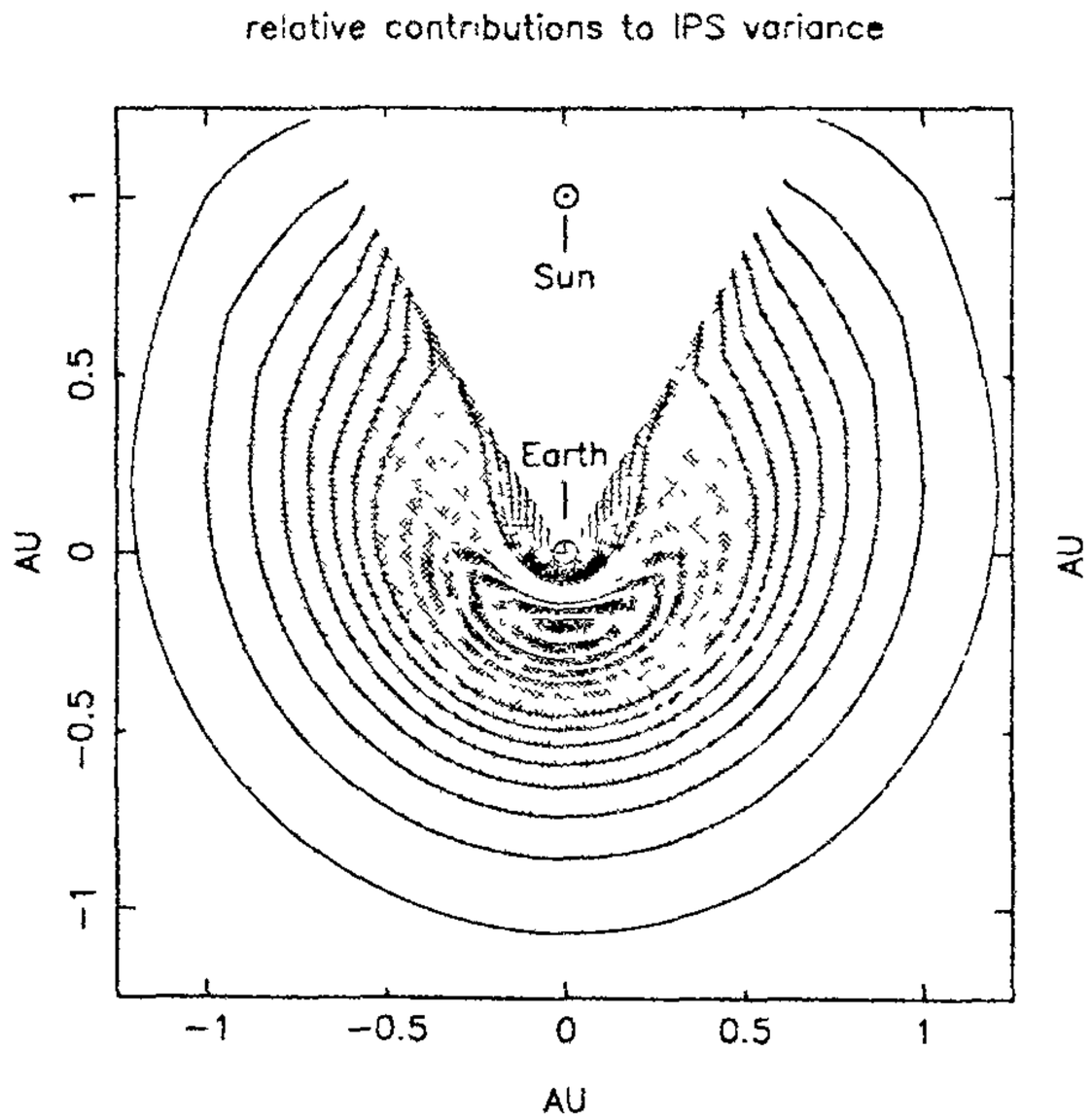

Figure 3. The scintillation weighting function showing the relative contributions of elements along the line of sight to the total value of g^2.

periods of about one year near sunspot maximum, when the magnetic poles are reversing their polarity, coronal holes always exist at each pole together with a small number at low latitudes. High-speed solar wind streams from coronal holes at low latitudes have been well studied by spacecraft located near the ecliptic plane and usually have speeds of roughly twice the average speed of about 400 km/s. Such streams often persist for several months and have been known to last for more than a year. In between the high speed streams are slower streams of higher density and the whole system rotates with the Sun generating an Archimedean spiral pattern with alternating zones of high and low density. A stable pattern of this type was present during January, 1993, and a sequence of maps showing a stream of high density as it approached the Earth from the east and then passed over to the west is shown in Figure 4. These maps, constructed by G. Woan[7], show the sky plotted in equatorial Hammer-Aitoff co-ordinates with the Sun's position indicated on the ecliptic. Values of g, averaged over $5^\circ \times 5^\circ$ pixels are presented in grey-scale over the range $0{\cdot}5 \leq g \leq 2$ and observations of roughly 1000 sources were used. The circles correspond to elongations (angular distances from the Sun) of 30° and 90°. Enhanced scintillation ($g > 1$) is shown darker, and the stream of high density first appears in the east on 22 January. As it approaches the Earth it covers an increasing area of sky, passing over the Earth on 25–26 January and then receding in the west. The approximate day to day location and longitudinal width of the steam are sketched in Figure 4. From the projected shape of the disturbance on 23–24 January, the stream has a larger angular width in ecliptic latitude than in longitude and is therefore a fan-shaped outflow. The rapid disappearance of the stream in the west, once it has passed over the Earth, is expected and is due to low density in the high speed stream following the enhanced density region in the corotating system. Reference to the scintillation weighting function shown in Figure 3 indicates that the resultant scintillation obtained by integration along the line of sight becomes dominated by the low density zone under these conditions, so the high density region is not seen for long after it has passed.

The interpretation of g-maps evidently demands some care when the dominant portion of the line of sight contains complex features having both high and low densities. In the absence of a theory of plasma turbulence for the small-scale irregularities causing turbulence we must rely upon empirical calibration for quantitative estimates of the mean plasma density. The most detailed work so far is that of Tappin[8] who compared simultaneous observations of scintillation and the mean density from *in-situ* spacecraft measurements. Tappin chose many occasions when the line of sight was covered by large-scale structures of high or low density. His database included both stable corotating streams and strong interplanetary shocks and he found that the relation $N = 9\,g^2$ cm^{-3} for the density gave a good fit to the observations under widely different conditions. There was a slight tendency for g to depend upon velocity gradients in the solar wind, but much the strongest correlation was with the mean density. It is desirable to check this calibration by *in-situ* observations of density turbulence, but spacecraft to date have not had the capability of measuring density fluctuations on the necessary short timescale.

Having obtained a suitable calibration it becomes possible to make quantitative estimates of the mean density provided conditions remain roughly constant over the relevant portion of the line of sight. It is also possible to compare the two-dimensional g-maps on the celestial sphere with numerical simulations for three-dimensional models, and hence to determine the global structure of large-scale disturbances. Applications of such model-fitting have been given by Tappin *et al.*[9,10]

The temporal evolution of corotating streams over a period of several years may conveniently be displayed by a series of compressed synoptic maps as illustrated in Figure 5. Each daily map is reduced to a strip showing the average value of g as a function of solar elongation, plotting the eastern and western halves of the sky separately. Information about the ecliptic latitude distribution is suppressed, but large scale corotating structures are readily identified by their characteristic 'herring-bone' appearance. Enhanced scintillation is indicated by the light bands, while the wider dark bands show low density associated with high-speed streams. One obvious corotating stream appears on Carrington rotations CR 1851 and 1852 as it makes successive crossings of the Earth around 19 January and 13 February, 1992. Simultaneous spacecraft measurements of plasma density by IMP-8, when available, have been found to agree well with the density estimated from scintillation which is plotted alongside the synoptic maps in Figure 5. The coronal hole associated with this high-speed stream is evident on the solar image for 13 January taken in the He 1083 nm line. This particular coronal hole was present for more than four rotations of the Sun and the synoptic maps show a close correspondence with its growth and decay during November 1991–May 1992.

Mapping interplanetary shocks

In addition to showing relatively stable features, g-maps often indicate the presence of short-lived transient disturbances moving radially outwards from the Sun. High density transients of this kind typically travel through the detection zone in two or three days, although exceptionally fast ones may be seen only once. When they pass over spacecraft, or the Earth, these transients

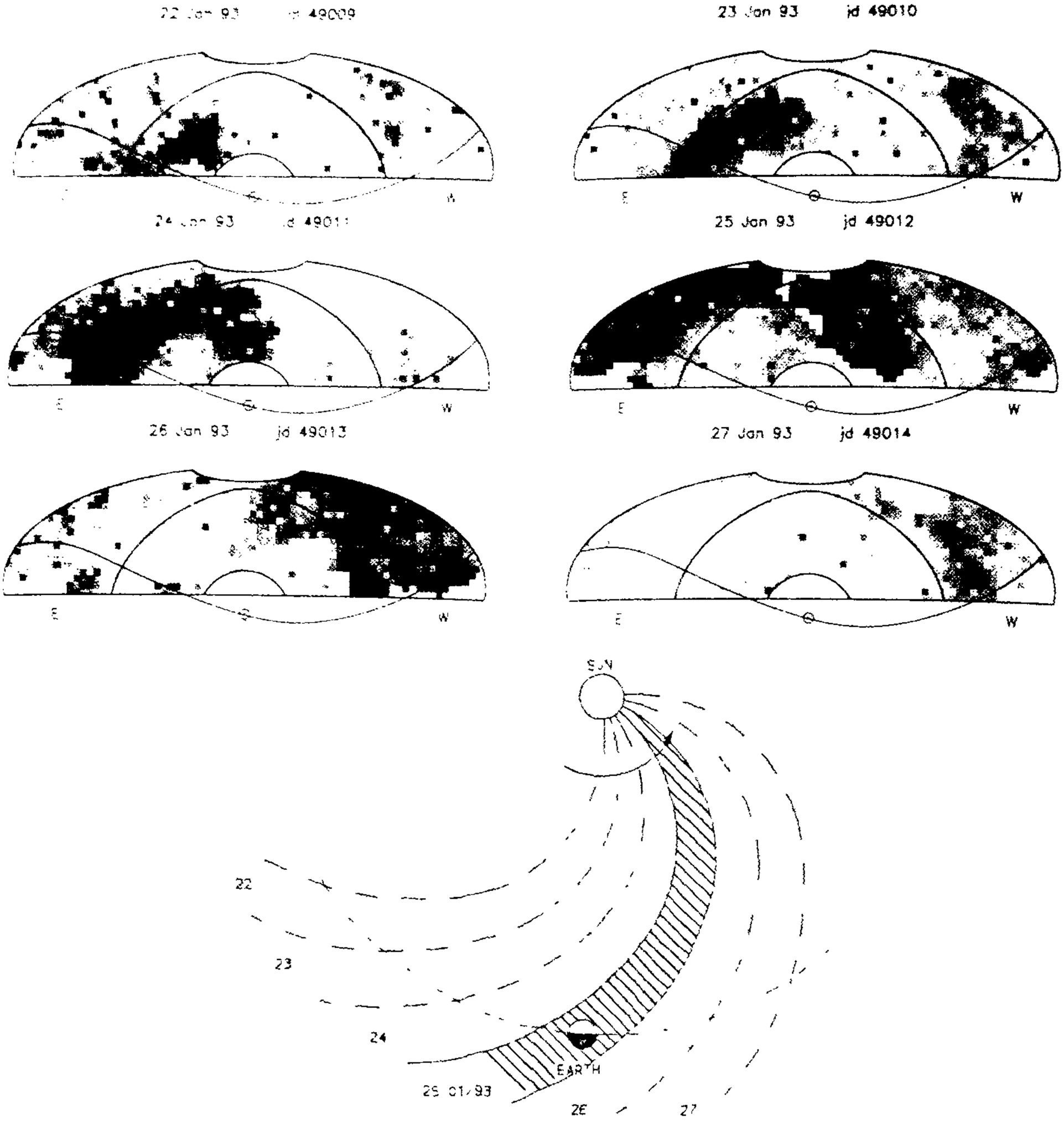

Figure 4. Daily *g*-maps in grey-scale for 22–27 January 1993 showing enhanced scintillation (dark) due to a corotating stream of high plasma density approaching Earth from the east and passing over to the west. The maps cover the whole sky in the declination range −20° to +70° and the Sun's position on the ecliptic is indicated.

are observed as interplanetary shocks and they compress the magnetosphere causing sudden changes in the geomagnetic field. Examples of interplanetary shocks detected on g-maps are shown in Figures 6 and 7. Because of their short duration they are not so easily seen on the compressed synoptic maps in Figure 5, but careful inspection shows white strips, without the slanting herring-bone pattern characteristic of corotating streams, and these are radially moving transients.

The most severe geomagnetic storms, and adverse 'space weather' conditions which can damage spacecraft systems, are caused by interplanetary shocks. Much effort has been given to understanding their solar origin with a view to predicting their occurrence. Until quite recently it was generally believed that they were caused by solar flares, the theory being that a sudden release of energy from stored magnetic fields in the solar corona could lead to impulsive heating and the acceleration of charged particles. Undoubtedly there is often a strong temporal correlation between major flare events and the initiation of interplanetary shocks, but solar flares are now no longer believed to be the prime cause as better observations using white light coronagraphs have shown that flares are secondary effects associated with the

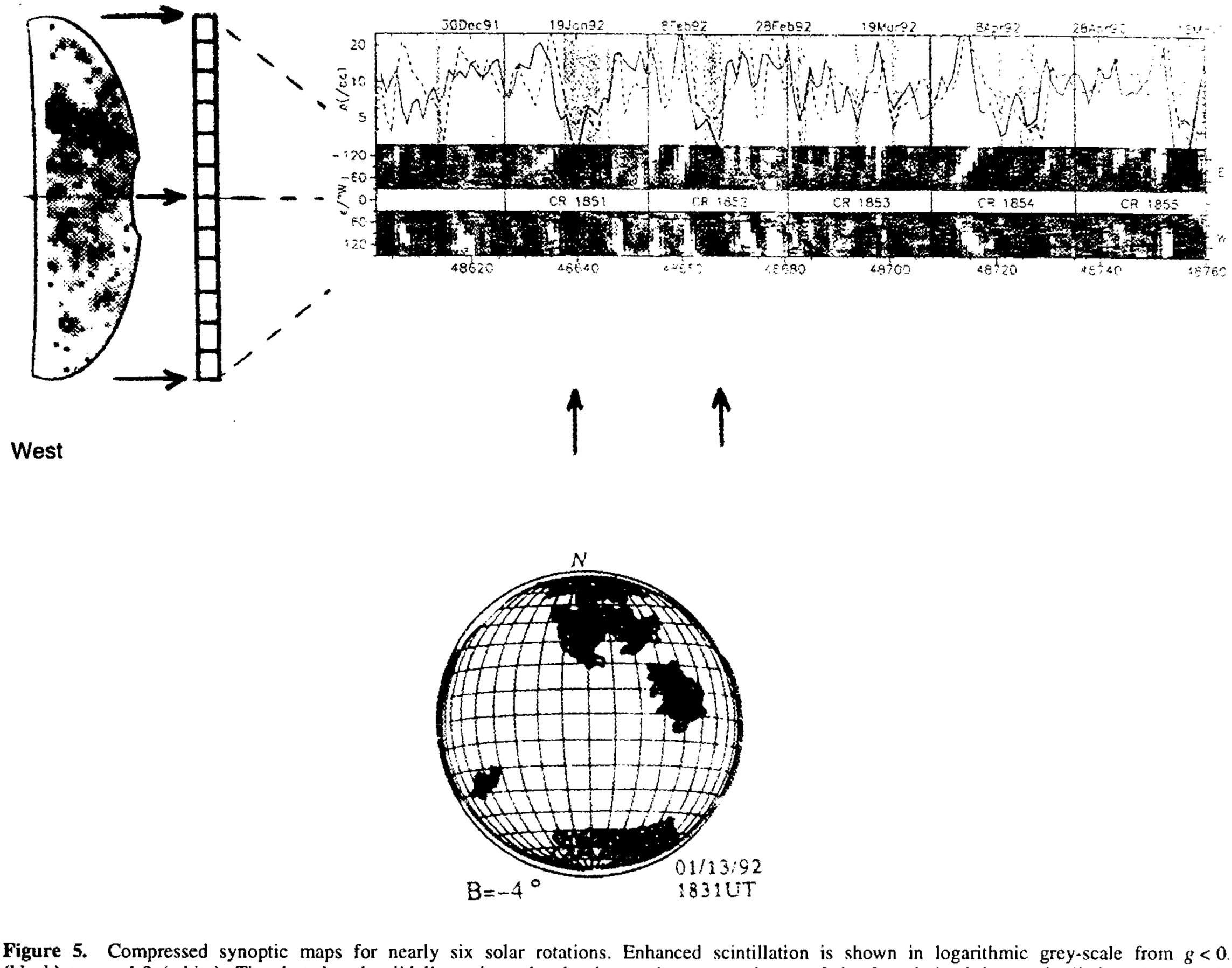

Figure 5. Compressed synoptic maps for nearly six solar rotations. Enhanced scintillation is shown in logarithmic grey-scale from $g < 0.77$ (black) to $g > 1.3$ (white). The dotted and solid lines show the density to the west and east of the Sun derived from scintillation. Arrows show a long-lived high speed stream of low density due to a prominent coronal hole.

eruption of solar prominences and coronal mass ejections. X-ray telescopes such as that on the Japanese satellite Yohkoh show that the outer corona is filled with loops and filaments held in place by the structure of the magnetic field. Especially at times of high solar activity, when the surface magnetic field is evolving rapidly, magnetic instabilities occur and magnetic loops erupt into space carrying entrained high density plasma. Associated solar flares usually occur at the 'footprints' of these loops, after the eruption has taken place, so they must be peripheral events. Strong correlations are found between coronal mass ejections and interplanetary shocks so it is now thought that the large-scale magnetic instabilities are the real causes of the disturbances[11].

Scintillation imaging of shocks confirms that solar flares are secondary effects but also adds new information suggesting that coronal mass ejection does not fully explain all the interplanetary phenomena associated with the strongest shocks. Because the shocks are moving radially our g-maps can be used to track them back to the Sun. In some cases we found large discrepancies between the position of flares 'confidently' assumed to be the causes of shocks and the actual locations estimated from our observations[12]. An interesting new result is a strong and statistically significant association between low-latitude coronal holes and the estimated shock-source positions on the Sun which suggests that strong interplanetary shocks may be caused by eruptions of high-speed wind from unstable coronal holes[13]. The acceleration mechanism of the solar wind is not yet known but is believed to be the deposition of energy from Alfvén waves high in the corona. At times of solar activity, there could be considerable variations in this supply of energy which would cause corresponding changes in the high-speed wind from coronal holes. This idea is supported by the fact that strong shocks are often followed by sustained high-speed outflows lasting for several days, a behaviour not expected to follow coronal mass ejections. It is possible, however, that the magnetic field evolution responsible for coronal

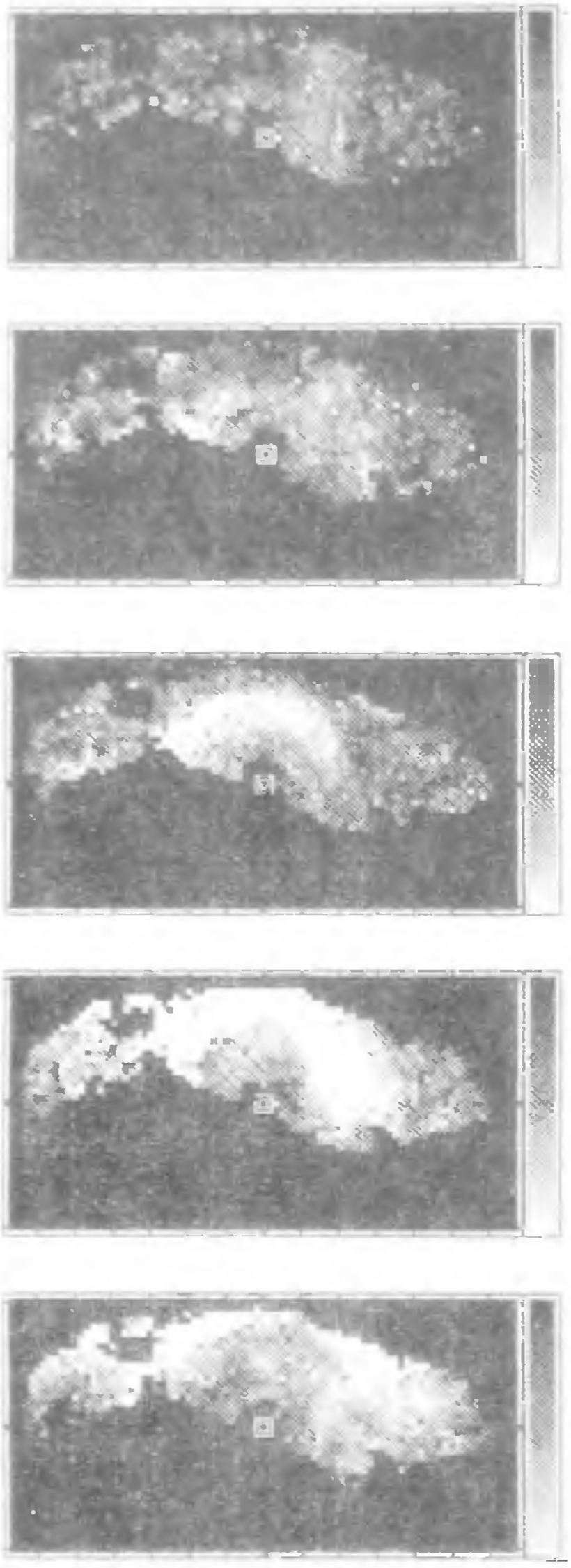

Figure 6. Whole sky g-maps for 26–30 September 1980 showing a major transient leaving the Sun above the ecliptic plane.

mass ejections could also change the geometry of nearby coronal hole outflows. There is evidence that a smaller divergence of magnetic field lines above coronal holes results in a faster wind. If the evolving field created less divergence the sudden acceleration of the solar wind could generate a shock in the interplanetary medium[14]. Disentangling cause and effect in the outer corona is clearly not a simple matter and the long-mistaken belief in the potency of solar flares should serve as a warning against drawing hasty inferences in solar-terrestrial physics.

Present problems and future prospects

Whilst scintillation mapping has great potential for routine monitoring of the near-Earth space environment and hence providing more accurate predictions of impending adverse conditions, there are two areas where improvements could be made. A single dedicated phased-array such as that at Cambridge can make only one map of interplanetary weather each day and intervals of 24 hours are too large for adequate tracking of fast disturbances moving radially. At an operating frequency near 100 MHz, disturbances are first seen at about one half the Sun–Earth distance and they could have arrived before a second map (needed to estimate their speed) became available. This problem could be overcome by establishing a global network of antennas at different longitudes. Four stations separated by 90° would provide maps with 6-hour delays. A second phased array operated by the Physical Research Laboratory at Ahmedabad should soon be in operation, and further arrays are under consideration in Mexico and Brazil, so this problem should be alleviated in the future.

Observations at a higher frequency, say 300 MHz, would enable disturbances to be mapped closer to the Sun, since the solar elongation at which scintillation saturates is reduced, but larger antennas are needed to achieve comparable maps owing to the reduction of source intensity. Significant improvements could be obtained only with considerably increased expenditure[15].

Another problem is contamination by ionospheric scintillation. Normally interplanetary scintillation is much faster than ionospheric scintillation and can be distinguished by high-pass filtering, but during geomagnetic storms ionospheric winds are enhanced causing rapid scintillation which is not easily separated from interplanetary scintillation. Contamination from this source is most pronounced at night, especially at high latitudes, and its effect can be seen in Figure 7. More sophisticated data-processing involving computation of the temporal power spectrum of the signal, combined with observations of sources having too large angular sizes to register interplanetary scintillation but responsive to ionospheric scintillation, should reduce this contamination. There would be an additional advantage as it is known that the power spectrum of interplanetary scintillation gives information on the solar wind speed[16]. Thus, in principle, it should be possible to compute maps of the wind speed as well as the plasma density which would add considerably to understanding the behaviour of interplanetary weather.

From the results that have been obtained so far it is evident that ground-based observations using dedicated radio telescopes can provide a valuable adjunct to direct *in-situ* measurements in space and the exploitation and

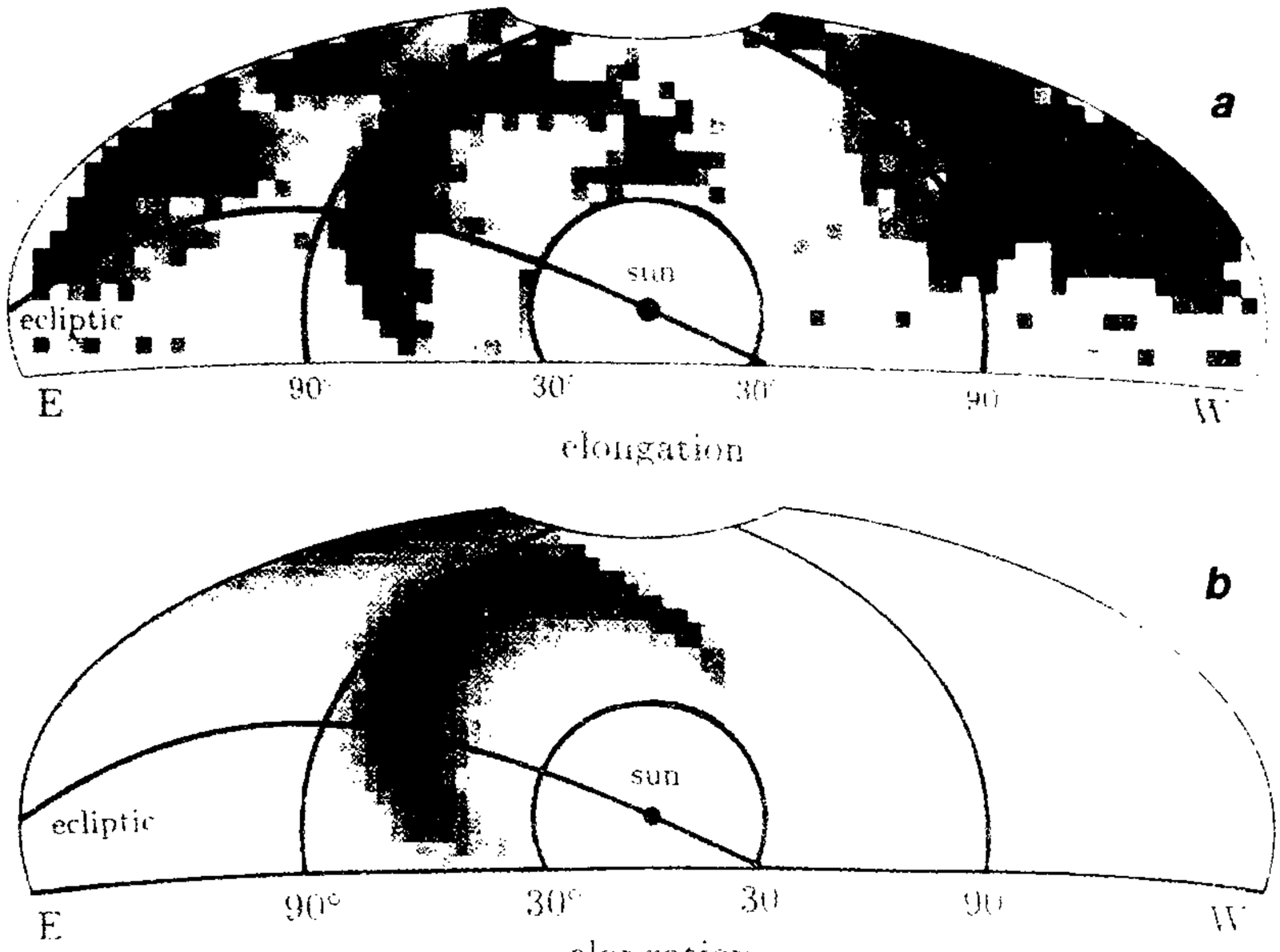

Figure 7. *a*, Map of a strong interplanetary shock to the east of the Sun observed near elongation 90° on 23 March 1991; *b*, Simulated *g*-map for a density enhancement of radial thickness 0.15 AU, angular width ± 40° and centred 20° above the ecliptic plane. This shock passed the spacecraft Ulysses on 25 March. Dark areas on the map at large elongations show contamination due to ionospheric scintillation.

further development of scintillation mapping should reap substantial rewards.

1. Hewish, A., Scott, P. F. and Wills, D., *Nature*, 1964, **203**, 1214.
2. Dennison, P. A. and Hewish, A., *Nature*, 1967, **213**, 343.
3. Kojima, M. and Kakinuma, T., *J. Geophys. Res.*, 1987, **92**, 7269.
4. Duffett-Smith, P. J., Purvis, A. and Hewish, A., *Mon. Not. R. Astron. Soc.*, 1980, **190**, 891.
5. Purvis, A., Tappin, S. J., Rees, W. G., Hewish, A. and Duffett-Smith, P. J., *Mon. Not. R. Astron. Soc.*, 1987, **229**, 589.
6. Readhead, A. C. S., Kemp, M. C. and Hewish, A., *Mon. Not. R. Astron. Soc.*, 1978, **185**, 207.
7. Woan, G., *Ann. Geophysicae*, 1994, in press.
8. Tappin, S. J., *Planet. Space Sci.*, 1986, **34**, 93.
9. Tappin, S. J., Hewish, A. and Gapper, G. R., *Planet. Space Sci.*, 1983, **31**, 1171.
10. Tappin, S. J., Hewish, A. and Gapper, G. R., *Planet. Space Sci.*, 1984, **32**, 1273.
11. Kahler, S. W., Moore, R. L., Kane, S. R. and Zirin, H., *Astrophys. J.*, 1988, **328**, 824.
12. Hewish, A. and Bravo, S., *Solar Phys.*, 1986, **106**, 185.
13. Hewish, A., Tappin, S. J. and Gapper, G. R., *Nature*, 1985, **314**, 137.
14. Bravo, S. and Peréz-Enriquez, R., *Rev. Mexicana Astron. Astrofis.*, 1994, **28**, 17.
15. Hewish, A. and Duffett-Smith, P. J., *Planet. Space Sci.*, 1987, **35**, 487.
16. Manoharan, P. K. and Ananthakrishnan, S., *Mon. Not. R. Astron. Soc.*, 1990, **244**, 691.

ACKNOWLEDGEMENTS. I thank Dr G. Woan for data shown in Figures 3, 4, 5 and 7. The Cambridge mapping project has received financial and technical support from the Space Environment Laboratory, Boulder, CO, the British Antarctic Survey and the Rutherford Appleton Laboratory.